Tungsten dust as a significant waste from a nuclear fusion reactor

Jaroslav STOKLASA, Lucie KARÁSKOVÁ NENADÁLOVÁ

Research Centre Řež (CVR), Hlavní 130, Husinec-Řež, 250 68, Czech Republic, e-mail: jaroslav.stoklasa@cvrez.cz

Abstract

During the normal operation of a tokamak (JET, ITER, EU DEMO), the highly durable tungsten armour on the inner surface of the reactor wears out. The sources of tungsten dust are investigated along with an assessment of the mechanism of its formation. Because of the processes involved, tungsten particles of different sizes are released. The tungsten material that is released is usually tritiated. Normally, it is removed from the reactor in the form of dust and treated as waste material. This valuable material should be separated from the radioactive tritium and recycled. To concentrate the tungsten, while simultaneously removing the tritium, it is possible to either use the molten salt oxidation technology or, alternatively, induction heating and melting, or a suitable combination thereof. This paper describes experimental testing of tungsten dust extraction using both technologies. The goal of the paper is to introduce the possibility that tungsten dust particles may be recycled using these methods, which seem to be very promising for the processing and recovery of this valuable waste.

Keywords: *Tungsten; Waste, Molten Salt Oxidation (MSO), Induction heating (IH), Size of particles*

Contents

1. Introduction

There are several open questions which need to be answered during the course of the conceptual design phase of the EU DEMO. Certain construction materials are likely to be used. New, and hopefully more suitable functional materials are under development. Materials have already been defined for the construction of parts of the device, in particular tungsten and steel. However, the amount and parameters of the waste dust generated inside the tokamak from these two materials can only be estimated.

The wear on the inner surface of a tokamak is caused by various factors. These are, for example, due to the kinetic energy of random neutral particles and their interaction with the construction and functional

materials, neutron irradiation, high heat and electromagnetic loads that induce significant thermal and mechanical stresses, as well as the combination or interaction of all these phenomena. All these processes and phenomena change the local entropy of the system. Moreover, the release of particles of different sizes, from single atoms, through clusters of atoms, grains, and even larger compact units has been observed.

The main purpose of this work was to search the literature for significant data on dust waste generation, select and merge it into information that is relevant to our experiments.

However, most of the work dealing with solid waste has not considered the entire basic chain between the production of the equipment material and the disposal of the waste. Our effort was to fill this gap by focusing more closely on the currently most important solid material stressed by fusion equipment operation and which is a significant source of waste, tungsten.

The topic of the article is focused on the use of MSO (Molten Salt Oxidation) and IH (Induction heating) technologies to reprocess tungsten dust from the fusion process. The research is directed towards solving two problems. The first phase is the separation of radioactive tritium from tungsten. The second phase is the reprocessing of the tungsten residue into a secondary raw material. In doing so, the potentially high variability in the properties of tungsten dust cannot be overlooked, as mentioned in various literature.

There are many unknowns with MSO and higher temperature induction heating and melting technology. The variability of powdered tungsten waste causes considerable complications in defining the parameters of both technologies. For these reasons, alternative technologies (for example, using LASER) are not considered in the literature review.

1.1. Origin of defects of various tungsten material

Normal operation of a nuclear fusion reactor causes wear to the highly durable tungsten (W) armour that results in the release of tungsten particles of different sizes. Some selected conditions and situations that may affect the formation of defects, faults, and consequently free W dust are tested.

Most of the works cited and other works known to us in the field of dust-producing fusion, are usually characterized by an interest in describing a single problem or a single device. Dust waste is usually described because of the operation of a tokamak or part of this. By selecting the papers, we have cited, the sources and origin of the dust, the change of material into waste, and the transformation of the waste that is subsequently accumulated are generally put into context.

Materials used as plasma facing components in future fusion reactors will be subjected to complex loading and various forms of interaction with low-Z species such as hydrogen isotopes and helium[1]. The divertor components will be among the most intensely loaded, as they will have to transfer nominal heat loads of up to 10 – 20 MW/m^2. While the plasma facing surface is irradiated by highly energetic deuterium, tritium and helium particles, coming from the burning plasma, the opposite side will be exposed to a coolant at elevated temperature. If the situation is not comprehensively addressed, there is a risk of damage or even destruction of the material.

The variability of tungsten dust is mainly related to the processes surrounding the formation of the dust. Its properties vary depending on the origin and places of dust generation, its physical properties and size also change throughout its journey in the fusion device. The source and quality of dust is affected by high temperatures and other variables at its origin (magnetic and electric fields, neutrons, gas pressures and composition, etc.). Dust sampling methods and techniques are equally important. For example, sampling of cold parts of equipment during maintenance or repair of equipment provides differences. Dust samples that have passed through the whole or part of the plant have a different quality if they have been collected in a cool and solid form, for example during continuous gas cleaning.

The tungsten released from the surface of the plasma facing components is usually tritiated. It is removed from the reactor as dust and is considered to be waste material. This valuable material[2] should be separated from the radioactive tritium and recycled.

The behaviour of W and W alloys in He gas at 720 °C was studied[1]. Pure W materials underwent only minor surface modification. W alloys experienced oxidation, preferentially of the alloying elements. The surface morphology of the ITER-qualified W, after helium exposure, was assessed. While the unexposed surface was virtually featureless, small scattered 'clusters' or 'nodules' appeared on the surface after exposure. They ranged from ~200 nm to ~2 μm in size; the majority were smaller than 1 μm. Examination through EDS (energy dispersive spectroscopy) on a TEM (Transmission electron microscopy) section indicated that the clusters were composed of tungsten only.

To overcome the intrinsic brittleness of tungsten, a tungsten fibre-reinforced tungsten-composite material (Wf/W) is being developed[3,4]. This composite addresses the brittleness of W by extrinsic toughening through the introduction of energy dissipation mechanisms[5,6]. These mechanisms are independent of the intrinsic material properties such as ductility.

High-velocity dust impacts on the wall represent the mechanism of wall damage and dust destruction. Normal W-on-W impact craters are studied[7] at target temperatures ranging from -100 °C to +400 °C, and impact speeds within 630 – 3100 m/s.

The release of W dust from compact surfaces can be initiated by mechanical and thermal processes. In the work by[8], the surface cracking features of tungsten armour, under thermal shock loads in an edge-localized mode (ELM), were investigated using computational fracture mechanics analysis. Based on the results, the threshold loading for cracking was found to be between 0.3 and 0.6 GW/m^2. The predicted threshold base temperature lies between 200 and 400 °C.

The study[9] summarizes the experimental results of pure heat load exposures, relevant to fusion, of different tungsten products in electron beam devices, JUDITH 1 and 2. The results show that the mechanical strength of the material has a significant influence on the formation and evolution of damage. In particular, recrystallisation and melting/solidification will make the material more prone to thermal shock and fatigue, accelerating the development of any damage.

The influence of the material characteristics of the raw powder on the resulting W part quality is discussed in[10] Thermal shock experiments on bulk W samples, produced using an additive manufacturing process, using the JUDITH 2 electron beam facility are described. W material, consolidated by means of laser powder bed fusion (LPBF), can survive highly intense thermal shock loads.

Damage to deformed double-forged pure tungsten has been studied in experimental simulations of ITER-like transient events with relevant surface heat load parameters[11]. The development of the surface morphology of the exposed targets as well as the cracking and swelling on the surface is discussed. Networks of micro- and macro-cracks develop on the surfaces of pure tungsten and tungsten-tantalum alloys due to surface irradiation with a heat load above the melting threshold. Transmission electron microscopy was used to determine which defects occur first during exposure and to compare the different effects of the JUDITH 1 and 2 machines[12]. No small-angle grain boundaries were formed, only line dislocations.

Chemical vapor deposition tungsten (CVD-W) is a promising material for plasma-facing materials[13]. Samples show good resistance to blistering and only a few micron-diameter blisters were observed at the fluences. It is suggested that the microstructure of the columnar grain and the texture of CVD-W samples help to suppress plasma-induced blistering, therefore reducing D retention. This can significantly affect the generation of W dust.

The influence of grain orientation and surface temperature on the growth of helium bubbles on a tungsten surface exposed to low-pressure helium plasma was investigated by a detailed Scanning Electron Microscope (SEM) imaging before and after plasma exposure[14]. From the analysis of nano-holes formed on the surface, the density and size of surface bubbles increase with higher temperatures and depending on the grain orientation.

The role of thermal stress- driven dislocation and grain boundary migration including grain orientation transitions on the tungsten surface under cyclic thermal shocks up to 1300 ºC is studied in[15]. The depth of these grain orientation transitions can reach several tens of micrometres, while the resulting surface roughness remains around 1 μm.

1.2. Effect of hydrogen on tungsten damage

An estimation of the hydrogen isotope flux imposed on fusion reactor wall components is important for material selection and to guarantee safe and economical operation of the reactor[16]. In all of the combined material systems investigated, the influence of the interface, meaning the change in material, on permeation flux is only minor compared to the much greater influence of the microstructure of the layer which strongly affects the permeability. The W layer permeability is several orders of magnitude higher than that of bulk W. Similarly, we can assume it has an effect on the movement of solid particles released.

The influence of grain boundaries (GBs) on the deuterium (D) transport and the formation of defects in nanocrystalline tungsten (W) films, deposited on a W substrate, was studied[17]. The D transport and retention was assessed through measuring the D depth profiles, after various exposure times, by nuclear reaction analysis (NRA) using an ^{3}He ion beam. The D concentration in the damaged area was highest in the sample with the smallest grain size. This shows that in nanocrystalline tungsten, irradiated at 27 ºC, the grain boundaries (GBs) do not improve the radiation resistance. Papers[10,18] describe a similar effect on tungsten and hydrogen capture induced by exposure to a mixture of deuterium and tritium.

1.3. Dust formation and accumulation

The primary source of dust is the areas within the equipment that are exposed in such a way that the surface of the material will be disturbed[19,20]. The quantity and quality parameters of the dust are affected by various mechanisms and processes, and these are discussed. Surface defects and structural changes of a preheated (550 ºC) tungsten plate after exposure to a plasma flux were studied[21]. Heating of the base of the tungsten plate, above the ductile–brittle transition temperature, made it possible to control the temperature gradient on its surface under pulsed plasma exposure but did not eliminate cracking of the surface. However, this significantly minimizes the amount of dust liberated from the surface of the tungsten plate under the influence of the plasma flux and almost no dust was observed. On the surface of the preheated tungsten plate, after exposure to the plasma flow, cracks with a width of no more than 1 μm were found and craters and blisters were also observed.

Neutron irradiation induced defect formation and recovery experiments have been extensively performed on tungsten[22,23]. Therefore, the activation energies required for interstitial, vacancy, cluster formation and migration are probably the most studied and accurate data available on irradiated tungsten. On the other hand, the macroscopic effects and mechanical properties have never been extensively investigated in detail[24]. Consequently, a large amount of technical data on a wider range of temperatures and doses, such as data on fracture mechanics, fatigue or creep, and radiation-induced cavity swelling, is still not available. It has been demonstrated that the high heat flux and thermal shock performance of tungsten and tungsten materials is due to a very complex interaction between a number of parameters which comprise, among others, loading conditions, thermal and mechanical properties, and microstructure.

Limits on dust and the tritium-inventory are an integral part of the ITER safety case and are fixed at 1 kg for tritium, 1,000 kg for easily mobilized dust and 11 kg (beryllium)/76 kg (tungsten) for dusts on hot surfaces[25]. For a reliable estimate of the dust inventory, an inspection should focus on areas within the container that have a greater probability to contain large concentrations of dust. It is usually argued that gravitational movement will tend to lead to the accumulation of dust particles on the floor of the vacuum vessel.

The experimental determination of the pull-off force for tungsten dust adhering to tungsten surfaces is described in[26]. The experimental pull-off force is nearly two orders of magnitude smaller than the predicted force from the contact mechanics models but is in strong agreement with the Van der Waals formula for spherical micron dust of various sizes. A theoretical explanation refers to the nanometre-scale surface roughness effects for rigid materials such as tungsten.

The shape and size distribution of the waste dust is influenced by the entire cycle of abrasion and wear of the materials. The physicochemical properties, phase composition, isotope abundance and ratio, radiation types and intensity, and mineralogical composition change. All the processes and ways in which dust may be generated are important. For this reason, the particle sizes range from clusters of atoms up to millimetres[27].

1.4. Summary of the consequences of the processes involved in the generation of W dust waste

The action of normal fusion reactor processes on compact primary tungsten material results in the generation of waste tungsten. Depending on the location of action of each process, the previously compact surface will range from disruption to varying depths to release of particles from the surface. Typically, a local combination of various physical, chemical, or radiological phenomena will occur that affect the compactness and integrity of an otherwise very resistant material.

Important physical and physicochemical phenomena include heat and thermal expansion, effects of temperature changes (crystallisation, phase transformation of components, formation of cavities), diffusion (especially of vacancies or gases), surface chemical reactions (hydrogen and metal), adsorption and desorption. Radiological phenomena include the transformation of isotopes by neutrons[28] and other radiation.

This result is grains of different sizes, shapes and dimensions. Grains have a variety of internal porosity and surface quality in micro dimensions. The surface of grains is not compact and has a large variation in imperfections. All of this influences the behaviour of the materials during further processing and reprocessing. It can be assumed that some material properties are imported from the initial production of the structural material before incorporation into the reactor. Other properties or parameters of the waste materials are related to the long-term stresses of sub-processes in a particular area or part of the fusion plant. The diversity of the appearance of (so far potential) waste dusts is shown in many publications in documented images, for example[3,12,17,28]. It can be assumed that a significant part of the waste dusts will have very similar appearance, diverse properties and behaviour when produced by ITER or EU DEMO facilities in the future.

2. Experimental methods for the reprocessing of tungsten waste dust

Within the EUROfusion project, various alternatives for the reprocessing of tungsten waste dust are being tested as part of the development and design of the EU DEMO. In view of the above literature, tungsten dusts of different grain sizes were used for the baseline tests.

Compact samples of tungsten dust with different granulometric compositions were prepared by pressing them into the shape of a small cylinder. Test pellets were prepared from tungsten particles with a grain size of 20 μm, 0.4 – 0.8 mm and 1 – 2 mm. A laboratory hydraulic press BSML 21 with a press force of 250 kN was used.

At the Research Centre Řež (CVR), tests are being carried out using the Molten Salt Oxidation technology or alternatively by the Induction Heating and Melting technology or a combination of them[29]. During the tailored sintering processes, the raw compacts will be densified to a degree that is sufficient for subsequent thermomechanical processing. The sintering of tungsten can be carried out between 2000 and 3000 °C under flowing hydrogen, or in a vacuum at similar temperatures, either by direct sintering (self-resistance heating) or indirect sintering (resistance element heating systems). The testing is performed in a vacuum chamber at increased temperatures. The samples will be further examined to determine the diffusible hydrogen volume. Based on the results, a decision can be made on possible recycling of tungsten dust particles generated by the proposed EU DEMO.

2.1. Molten Salt Oxidation

Molten Salt Oxidation is a technology that utilizes flameless oxidation in salt melt[29]. It is an alternative to the conventional treatment, i.e., the decomposition of hazardous and radioactive waste. The waste is directed below the surface of the molten salt together with an oxidizing agent (O_2, air) if the W dust contains organic waste or another combustible component. For the process operation to be optimal, it needs to take place at the interface of the three phases. The principle underlying the technology is the reprocessing of suitable materials through the distribution of the materials into their liquid and gaseous phases. At a pre-defined elevated temperature, solid and liquid materials are caught within the alkaline

molten salt and separated from the gaseous products. Heavy metals and radionuclides are captured within the salt, which can then be reprocessed.

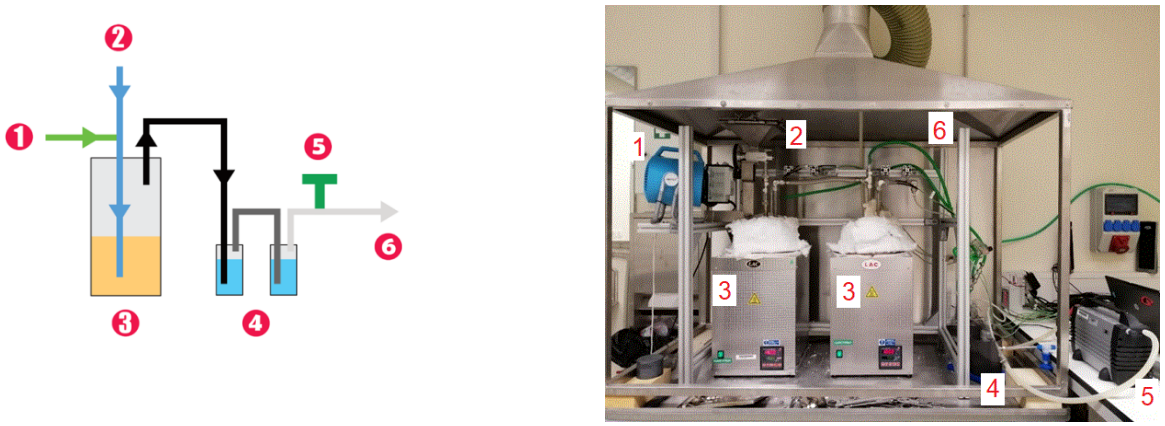

Figure 1: Scheme and photo of the MSO laboratory apparatus, 1 - propellant (Air), 2 – pellet dosing device, 3 – reactor vessel, 4 - water bubblers, 5 - vacuum pump, 6 – ventilation.

The scheme of the MSO laboratory apparatus is shown in Figure 1, where inlet No. 1 is for dosing tungsten waste, inlet No. 2 is intended for air. Water-soluble gases are captured in bubblers No. 4, and vacuum pump No. 5 facilitates the flow of gases and vapours from reactor No. 3. The water from the bubblers is analysed. The content of the deuterium water was analysed by Attenuated Total Reflection Fourier Transformed Infrared Spectrometry (ATR-FTIR). The tritiated water contents was analysed by the Liquid Scintillation Counting method (LSC).

Various grain size fractions of tungsten dust and their mixtures are tested, ranging from the very fine fractions (below 20 μm) through medium sizes (0.4 – 0.8 mm) to grain sizes of 1 – 2 mm. These tungsten samples are used either directly untreated or treated to contain either deuterium water or tritiated water in defined amounts. The samples are dosed continuously or in batches of grams into the reactor.

The details surrounding the hydrogen tests with deuterium and tritiated tungsten are beyond the scope of this article. However, it should be emphasized that no hydrogen remains with the tungsten in the molten salt at the end of the MSO process.

For our reactor tests, carbonates of alkali metals (Na, K, Li) or their mixtures are used. These salts are melted at different monitored temperatures and tungsten dust samples are dosed into these salts in different ways. An example of test parameters is the use of Li_2CO_3 maintained at 800 °C, the grain fraction of tungsten dust dosed continuously or in batches of units of grams. 180 g of carbonate alkali salts were used. The temperature was maintained for 30 min followed by a rapid cooling.

Preliminary tests showed that all the metallic tungsten that was dosed could be converted to oxides and oxide hydrates during the MSO process. Nevertheless, the passage of tungsten grains through the molten salt was observed.

In separating the trapped tungsten products from the carbonate salt, the alkaline carbonates were separated first. This was done in such a way that neither the solid W nor the tungsten salts were lost. This was a procedure that alternated between washing with water and washing with suitable acids (HCl, H_2SO_4, HNO_3). The dissolved products were evaporated and precipitated. The solid product with tungsten was collected. The removed soluble salts were checked for tungsten content. The separated tungsten solid phase was washed several times with demineralized water and, in the final stage, dried.

X-ray Diffraction (XRD) analysis of the samples that underwent the MSO process was performed. A PANalytical X'Pert Pro powder diffractometer was used for the measurements.

A Scanning Electron Microscope SEM Lyra 3, from Tescan, and an Energy Dispersive X-ray Spectrometer (EDX), from Oxford Instruments, were used to verify the particle size distribution in the sample. Tungsten with a declared particle size in the range of 0.5 – 2 μm was used for the tests. This is the smallest fraction of tungsten that has undergone the MSO process and all washing steps. Baseline measurements[30] were recorded. The sample was prepared according to the SUJB certified methodology[31]. The following parameters were used for the measurements: Depth-mode, accelerating voltage of 25 kV, current of 1 – 5 nA at beam footprint <50 nm, working distance of 9 mm. A backscattered electron (BSE) detector was used during the measurements.

2.2. Induction heating

Cold crucible induction melting is an innovative process that can be used to melt high temperature reactive materials[32]. A water-cooled segmented crucible is used instead of a ceramic crucible to avoid any kind of reaction between the charge and the crucible. A magnetic field, generated by an external coil, penetrates the slits of the crucible and induces currents which melt the charge through Joule heating.

Induction heating can be performed using a direct or indirect method[33]. With direct induction heating, joule losses are generated directly in the object that is being heated. Indirect induction heating entails heating an element which can be heated by induction and transferring that heat by conduction to the workpiece. Various methods of induction heating are used to achieve high temperatures in many types of materials, for example in metallurgy or semiconductor preparation[34]. It is also used in the study of the interactions of materials with radioactive molten corium[35] and in studies of the behaviour of highly refractory materials, where it can be used to describe phase phenomena at high temperatures[36].

Sintering of tungsten powders can take place at relatively low temperatures (1000 – 1200 °C) in a suitable atmosphere. The study[37] describes sintering without alloying additives using a closed reaction space and water saturated with hydrogen and steam.

The advantage of induction heating is the possibility of reaching very high temperatures (above 2000 °C) at which all the hydrogen, for example from tritiated waste, can be released in a suitable atmosphere.

Tests of direct and indirect heating in a cold crucible with powdered tungsten were carried out.

Different types of samples were prepared: with the addition of demineralized water, with the addition of tritium water, and without any water addition. Furthermore, samples prepared at ENEA Frascati were also tested. These samples were prepared using tungsten dust into which hydrogen was incorporated at high pressure and temperature (with a final concentration of 15 ppm of hydrogen). The sample in the carbon crucible was heated indirectly by IH in an inert argon atmosphere. At a temperature of about 1300 °C the hydrogen was removed.

The crucible was heated by electromagnetic induction, and the sample directly heated. In order to avoid oxidation of the tungsten, the operation took place in an argon-inert atmosphere. The sample was produced by compressing a mixture with a grain size of 20 μm to 2 mm. It was sintered at 1730 °C by direct induction heating, with a layer of ZrO_2 present around the sample to form a safety crucible and prevent oxidation by the surrounding atmospheric air.

3. Test results

3.1. Results MSO

The powdered tungsten underwent the MSO process and was used during the powder dosing trials at the CVR facility. A significant portion of the sample was oxidized in the process and dissolved in the carbonate melt.

The inputs and outputs from experimental work with tungsten fractions in molten salts are shown in Table 1. The solid product was obtained after dissolving the cooled carbonate salt from the MSO reactor and separating the solutes by decantation and washing.

Table 1: Inputs and outputs of solid components of experimental work with tungsten fraction in molten carbonate alkali salts

Fraction W	**≤ 20 µm**	**0.4 – 0.8 mm**	**1 – 2 mm**	**≤ 20 µm**	**0.4 – 0.8 mm**	**1 – 2 mm**	**≤ 20 µm**	**0.4 – 0.8 mm**	**1 – 2 mm**
	Na_2CO_3; 950 °C			**Li_2CO_3; 800 °C**			**K_2CO_3; 980 °C**		
Input W (g)	20.697	20.104	20.384	19.60	20.00	20.00	20.047	20.505	20.251
Metal W (g)	0.631	8.852	10.199	3.101	19.322	19.432	1.328	9.395	12.963
$WO_3.xH_2O$ (g)	13.724	2.553	5.428	18.277	0.755	5.358	15.191	4.339	0.412

Depending on the process setup, 30 to 80% solid tungsten accumulates at the bottom of the reactor. A maximum of 97.1% was measured.

The degree of tungsten oxidation and metal W loss are proportional to the granulation: directly proportional to the total surface area of the grains but inversely proportional to the individual grain diameter, as can be seen in Table 1. However, with appropriate dosing and oxidation conditions, 100% of the solid tungsten can be dissolved. For further work, it is advantageous to capture solid tungsten, which can be reprocessed, for example, by induction heating.

An XRD analysis of metal W grain size 20 µm treated by MSO is shown in Figure 2.

The solid products were used for further measurements. A summary of the basic measurements on the Lyra 3 scanning electron microscope is given in Table 2. Figure 3 shows tungsten grains with the sizes of 0.4 to 0.8 mm from a sample that underwent the MSO process. It is the solid residue left after the removal of the water-soluble salts. Figures 4 and 5 show examples of fine tungsten particle clustering, where an irregularly shaped particle is expressed as the equivalent circle diameter (ECD) of the same area. The spread-out particles also tend to form more complicated clusters of some stability, as seen in Figure 6.

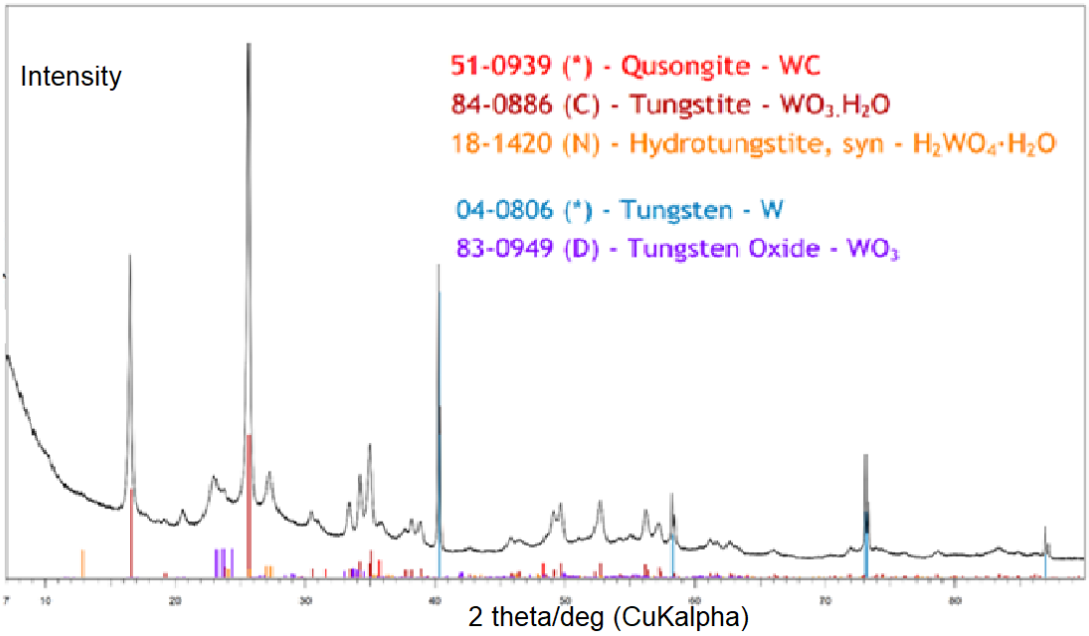

Figure 2: XRD analysis of metal W grain size 20 µm from the MSO reactor. The molten salt was Li_2CO_3 at 800 °C.

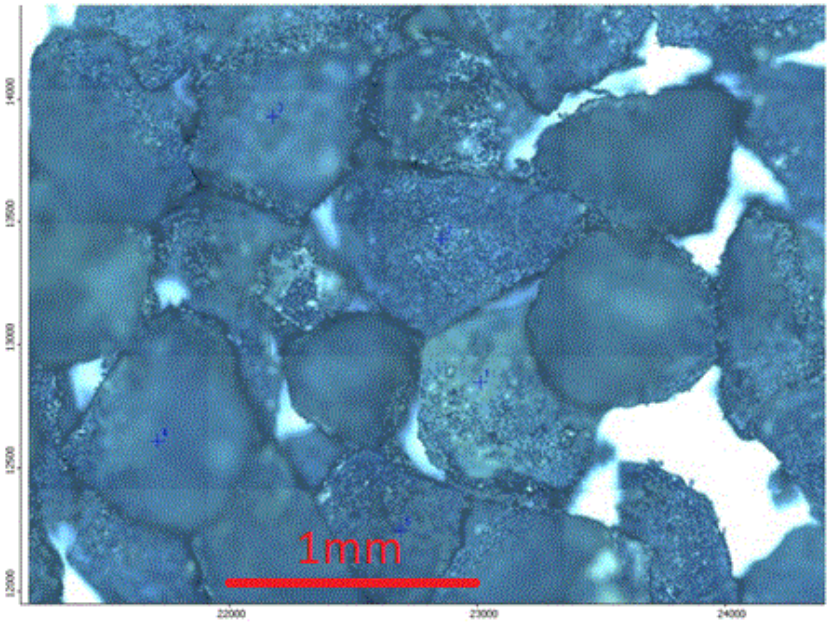

Figure 3: A photograph of the final sample of W with a grain size from 0.4-0.8 mm with molten Li_2CO_3 using Raman spectroscopy.

***Table 2: Summary of basic measurements of the smallest fraction of tungsten*.**

	Area 1	**Area 2**
Analysis time (min)	39	38
Number of particles detected and analysed	54	42
Field area (μm^2)	1600	1600
Total analysed area (μm^2)	40700	58500
Total area of particles analysed (μm^2)	41.7	42.3
Proportion of detected particles from the analyzed area (%)	0.1	0.07

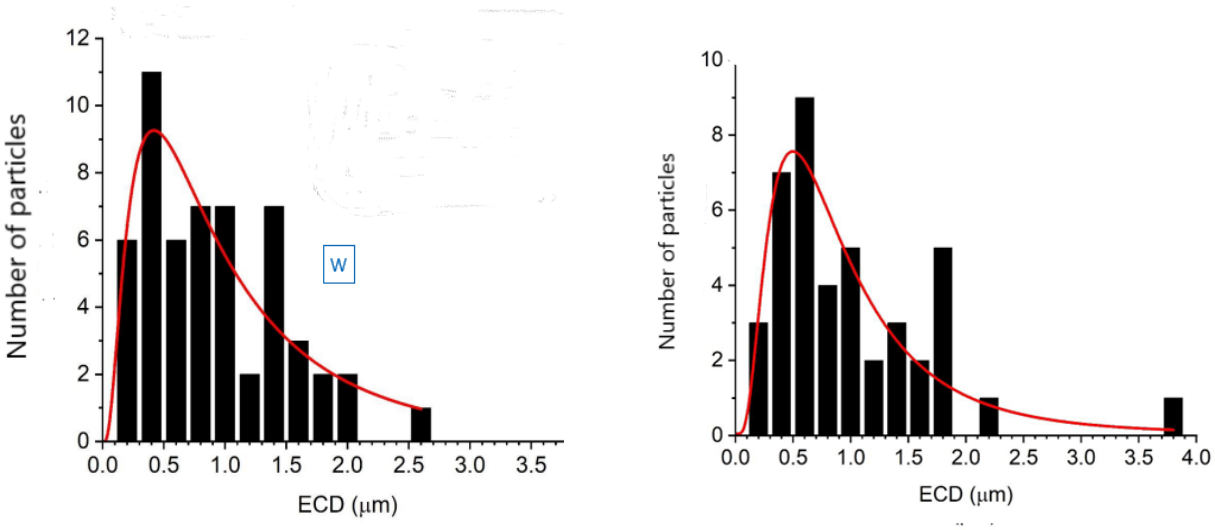

Figure 4 and 5: Tungsten particle size distribution in analysis area 1 (left) and analysis area 2 (right).

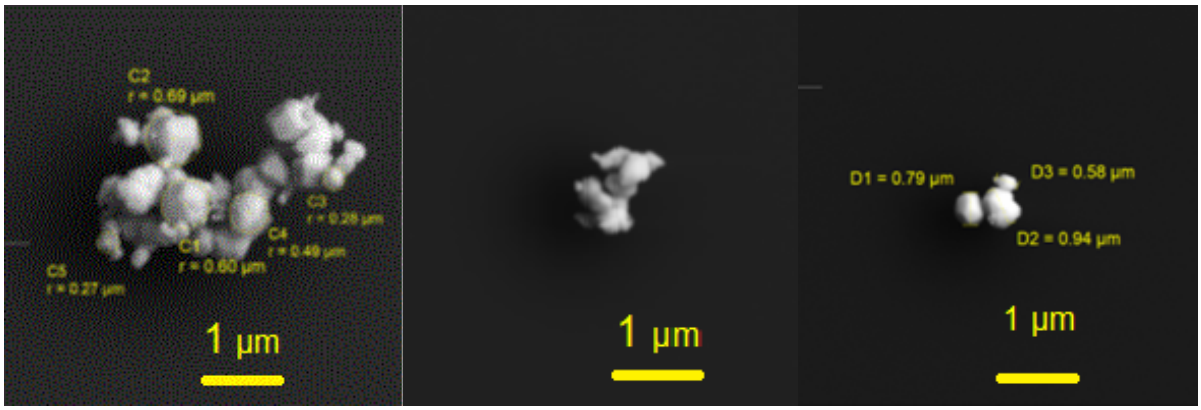

Figure 6: A cluster of tungsten particles shown in the BSE mode; the photograph is complemented by measurements of the radii of individual particles that make up the cluster in the image.

3.2. Results of induction heating of tungsten powder

Several types of heating (direct, indirect) of samples in different atmospheres were performed. Compact samples were prepared from different types of tungsten powders.

A view of the cold crucible and induction system before and after heating the sample is shown in Figure 7. The sample is heated directly by electromagnetic induction in an argon-inert atmosphere. The cold crucible for the W sample was coated with a layer of zirconium oxide.

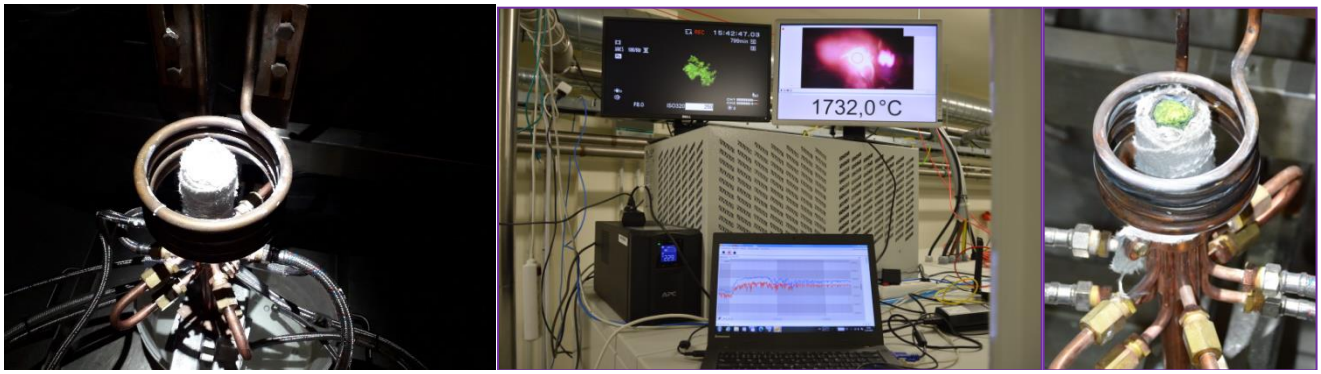

Figure 7: A view of the induction system before heating (left) and after heating (right), the middle picture shows the CC control system.

Figure 8 shows a cross-section of a sintered tungsten sample. During the heating process, some grain bonding and grain growth occurred. The final sintered material is compact and very strong.

Direct induction heating in an air atmosphere was also performed. A coating of oxides began to form on the surface of the sample. After cooling, the surface colors were stable. Depending on the ambient conditions, especially air flow, cooling time and temperature, they were blue or yellow in color. With prolonged exposure to air oxygen, the oxide formation proceeded to the depth of the sample.

Figure 8: Cut through the sintered tungsten sample.

Figure 9 shows the result of tungsten oxide formation in a wide range of color shades from green to blue and ochre. The variability in color is related to the cooling behavior of the sample in air.

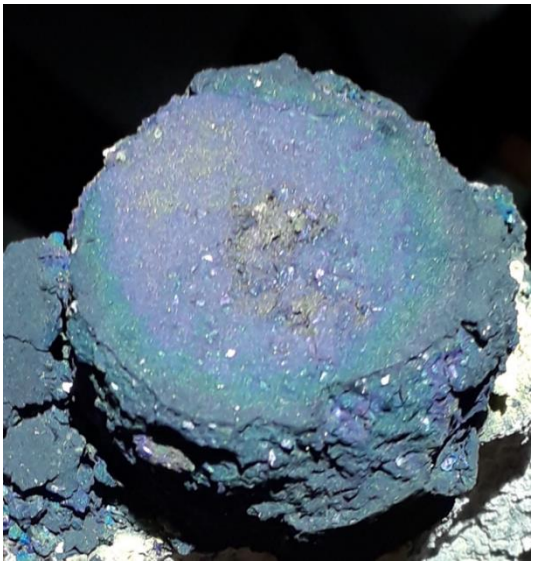

Figure 9: Variable color of tungsten oxides after direct induction heating in air, pressed tungsten powder

4. Discussion of experiments

4.1. Discussion MSO

It has been found that going through the MSO process does not always result in full oxidation of tungsten. The input fractions of W and the output components, which were metallic tungsten and hydrated tungsten oxide, were monitored. Comparison of the mass of solid products in MSO processes shows the possibility of passing tungsten grains without dissolution. They have resistance to highly aggressive molten salts at the appropriate temperature. The granulation affects the degree of tungsten oxidation.

The material that gravitationally settles and accumulates in the lower part of the reactor is tungsten grains completely depleted of hydrogen (tritium) content. With a suitable combination of process parameters and molten salt composition, it will be possible to achieve higher yields of solid tungsten grains. This will be influenced mainly by the temperature, viscosity, wettability, and surface tension of the molten salt. It will also depend on the grain size and as yet unspecified quality of the grain surface. The cited and other literature mentions a variety of qualitative parameters and is still ambiguous on this issue.

It will also be affected by the way the waste material is fed into the MSO process. There are also noticeable differences for different molten alkaline carbonate salts.

4.2. Discussion IH

The IH technology seems to be very promising for the compaction of waste tungsten dust. Care must be taken to avoid oxidation of the metal. Logically, it is suggested to carry out heating with excess hydrogen (tritium) in the sample environment. It is likely that the tritium present in the sample may not be sufficient to prevent oxidation. Oxidation is also prevented by working in an inert gas or vacuum environment, which offers opportunities to perform further experiments leading to an optimal setup of the whole process.

5. Conclusions

The work is an introduction to the complex and up to know only marginally addressed issue of fusion waste. Our intention was to determine some parameters for further research on the treatment of tungsten waste generated during fusion. During the research work, some sources of W dust were identified. The places or origins of their probable production were monitored mainly with respect to the future EU DEMO devices. A possible mechanism for the formation of this valuable waste is also indicated.

This work describes experimental tests carried out on tungsten dust using both the MSO and induction heating methods in a cold crucible with tungsten dust. The changes in tungsten grains after both types of experiments were evaluated. The samples tested are close to the predicted EU DEMO tungsten waste dusts that were described in the literature review, with emphasis on grain size and shape.

Both technologies can separate tungsten from tritium very efficiently. Using MSO technology, tritium is captured in the form of tritiated water. Bubbling in water has a very high capture efficiency. No tritium in the cooled carbonate salt or residual tungsten is indicated at the end of the test. The suitability of using carbonates (Na, K, Li) is well demonstrated.

If the tungsten is not oxidized during the use of the MSO technology, solid tungsten will accumulate at the bottom of the reactor, depending on the density difference between the salt and grains of tungsten. Through appropriate dissolution processes, this tungsten can be separated from the salt, cleaned and further processed. Pure tungsten can also be obtained from used salts with soluble and oxidized forms of tungsten using suitable physicochemical processes.

When using the IH technology, it is necessary to remove the tritium gas from the process either in vacuum or in a mixture with an inert gas, depending on the setting of the IH technology parameters. The first option is to treat the tritium in a similar way to the treatment of gases leaving experimental tokamaks, where the tritium is separated from the other gases. The second option is to oxidise the escaping tritium appropriately, capture it in the form of tritiated water and prepare it for reprocessing as a liquid.

The sintering of tungsten dust grains by induction heating results in their aggregation and a further increase in grain size. The sample is compact and much stronger than after pressing.

To verify the efficiency of hydrogen (tritium) removal from tungsten dust, it will be necessary to work with higher concentrations of hydrogen bound in tungsten and at different temperatures. Research into

both technologies will continue and will focus on optimization of the process flow. This will include function even assuming yet undefined waste variability but also the possibility of linking the two technologies in a future potential plant.

Knowing the more precise parameters of the waste that will be produced by ITER and EU DEMO will allow both facilities to adapt quantitatively and qualitatively to fusion waste.

The possibility to recycle tungsten dust particles using these individual methods (IH and MSO) or a combination of them appears to be very promising as a method to treat this valuable waste so that it can be reused separately as both high-quality raw materials (tritium or tungsten).

Acknowledgment

This work has been carried out within the framework of the EUROfusion Consortium, funded by the European Union via the Euratom Research and Training Programme (Grant Agreement No 101052200 — EUROfusion). However, the views and opinions expressed are those of the author(s) only and do not necessarily reflect those of the European Union or the European Commission. Neither the European Union nor the European Commission can be held responsible for them.

The implementation of activities described in the Roadmap to Fusion during Horizon Europe through a joint programme of the members of the EUROfusion consortium has been also supported by the Ministry of Education, Youth and Sports (MEYS) of the Czech Republic project number 9D22001.

The presented results were obtained using the CICRR infrastructure, which is financially supported by the Ministry of Education, Youth and Sports - project LM2023041.

References

1. J. Matějíček, M. Vilémová, H. Hadraba, F. Di Gabriele, I. Kuběna, E. Kolíbalová, J. Michalička, J. Čech, A. Jäger, Behavior of W-based materials in hot helium gas, Nuclear Materials and Energy 9 (2016) 405 – 410. https://doi.org/10.1016/j.nme.2016.03.009
2. E. Lassner, W-D. Schubert: Tungsten - Properties, Chemistry, Technology of the Element, Alloys, and Chemical Compounds, Kluwer Academic/ Plenum Publishers, New York (1999). https://doi.org/10.1007/978-1-4615-4907-9
3. R. Neu, J. Riesch, A.v. Müller, M. Balden, J.W. Coenen, H. Gietl, T. Höschen, M. Li, S. Wurster, J.-H. You, Tungsten fibre-reinforced composites for advanced plasma facing components, Nuclear Materials and Energy 12 (2017) 1308 – 1313. https://doi.org/10.1016/j.nme.2016.10.018
4. Yiran Mao, Jan Coenen b, Sree Sistla, Chao Liu, Alexis Terra, Xiaoyue Tan, Johann Riesch, Till Hoeschen, Yucheng Wu, Christoph Broeckmann, Christian Linsmeier, Design of tungsten fiber-reinforced tungsten composites with porous matrix, Materials Science and Engineering: A 817 (2021) 141361. https://doi.org/10.1016/j.msea.2021.141361
5. J. Riesch, J.-Y. Buffiere, T. Höschen, M. Scheel, Ch. Linsmeier, J.-H. You, Crack bridging in as-fabricated and embrittled tungsten single fibre-reinforced tungsten composites shown by a novel in-situ high energy synchrotron tomography bending test, Nuclear Materials and Energy 15 (2018) 1 – 12. https://doi.org/10.1016/j.nme.2018.03.007
6. B. Jasper, S. Schoenen, J. Du, T. Hoeschen, F. Koch, Ch. Linsmeier, R. Neu d, J. Riesch, A. Terra, J.W. Coenen, Behavior of tungsten fiber-reinforced tungsten based on single fiber push-out study, Nuclear Materials and Energy 9 (2016) 416 – 421. https://doi.org/10.1016/j.nme.2016.04.010
7. M. DeAngeli, P. Tolias, F. Suzuki-Vidal, D. Ripamonti, T. Ringrose, H. Doyle, G. Daminelli, J. Shadbolt, P. Jarvis, M. DeAngeli: Normal high velocity solid dust impacts on tiles of tokamak-relevant temperature, Nuclear Materials and Energy 41 (2024)101735. https://doi.org/10.1016/j.nme.2024.101735

8. Muyuan Li, Jeong-Ha You, Cracking behavior of tungsten armor under ELM-like thermal shockloads II: A revised prediction for crack appearance map, Nuclear Materials and Energy 9 (2016) 598 – 603. https://doi.org/10.1016/j.nme.2016.02.001
9. M. Wirtz, J. Linke, Th. Loewenhoff, G. Pintsuk, I. Uytdenhouwen, Transient heat load challenges for plasma-facing materials during long-term operation, Nuclear Materials and Energy 12 (2017) 148 – 155. https://doi.org/10.1016/j.nme.2016.12.024
10. A.v. Müller, D. Dorow-Gerspach, M. Balden a, M. Binder, B. Buschmann, B. Curzadd, T. Loewenhoff, R. Neu, G. Schlick, J.H. You, Progress in additive manufacturing of pure tungsten for plasma-facing component applications, Journal of Nuclear Materials 566 (2022) 153760. https://doi.org/10.1016/j.jnucmat.2022.153760
11. V.A. Makhlai, I.E. Garkusha a, J. Linke, S.V. Malykhin, N.N. Aksenov, O.V. Byrka, S.S. Herashchenko, S.V. Surovitskiy, M. Wirtz, Damaging of tungsten and tungsten–tantalum alloy exposed in ITER ELM-like conditions, Nuclear Materials and Energy 9 (2016) 116 – 122. https://doi.org/10.1016/j.nme.2016.04.001
12. W. Van Renterghem, I. Uytdenhouwen, Th. Loewenhoff, M. Wirtz, TEM analysis of recrystallized double forged tungsten after exposure in JUDITH 1 and JUDITH 2, Nuclear Materials and Energy 9 (2016) 484 – 489. https://doi.org/10.1016/j.nme.2016.04.003
13. Hao Yin, Long Cheng, Xuexi Zhang, Hong Zhang, Wangguo Guo, Yue Yuan, Binyou Yan, Peng Wang, Guang-Hong Lu: Surface blistering and deuterium retention in chemical vapor deposition tungsten exposed to deuterium plasma, Nuclear Materials and Energy 37 (2023) 101536. https://doi.org/10.1016/j.nme.2023.101536
14. M. Alfazzaa, F. Pappalardo, A. Campos, G. Cartry, M. Minissale, C. Martin: Grain orientation and temperature dependences of bubbles at tungsten surfaces upon helium plasma exposure, Nuclear Materials and Energy 42 (March 2025) 101883. https://doi.org/10.1016/j.nme.2025.101883
15. M-C. Ren, Y-F. Nie, H-Q. Wang, Y. Yuan, F. Feng, Y-Y. Lian, H. Yin, L. Cheng, D-Q. Shi, G-H. Lu: Role of thermal stress-driven dislocation and low-angle grain boundary migration in surface plastic deformation and grain orientation evolution of tungsten under thermal shock International Journal of Plasticity 184 (January 2025) 104205. https://doi.org/10.1016/j.ijplas.2024.104205
16. A. Houben, M. Rasiński, S. Brezinsek, Ch. Linsmeier: Hydrogen isotope permeation through interfaces and permeability of tungsten layers, Nuclear Materials and Energy 37 (2023) 101518. https://doi.org/10.1016/j.nme.2023.101518
17. S. Markelj, T. Schwarz-Selinger, M. Kelemen, E. Punzón-Quijorna, J. Zavašnik, A. Šestan, D. Dellasega, G. Alberti, M. Passoni: The effect of nanocrystalline microstructure on deuterium transport in displacement damaged tungsten, Nuclear Materials and Energy 37 (2023) 101509. https://doi.org/10.1016/j.nme.2023.101509
18. V.Kh. Alimov, Y. Torikai, Y. Hatano, T. Schwarz-Selinger, Tritium retention in displacement-damaged tungsten exposed to deuterium-tritium gas mixture at elevated temperatures, Fusion Engineering and Design 162 (2021) 112100. https://doi.org/10.1016/j.fusengdes.2020.112100.
19. Y. Corre, M-H. Aumeunier, A. Durif, J. Gaspar, K. Krieger, T. Loewenhoff, M. Richou, S. Ratynskaia, Q. Tichit, Y. Anquetin, R. Dejarnac, M. Diez, L. Dubus, M. Firdaouss, J. Gerardin, A. Grosjean, J.P. Gunn, T. Loarer, P. Maget, C. Martin, K. Paschalidis, E. Tsitrone, M. Wirtz, the WEST team, Testing of ITER-grade Plasma Facing Units in the WEST tokamak: progress in understanding heat loading and damage mechanisms, Nuclear Materials and Energy 17 (2023) 101546. https://doi.org/10.1016/j.nme.2023.101546
20. C. Arnas, A. Campos, M. Diez, S. Peillon, C. Martin, K. Hassouni, A. Michau, E. Bernard, N. Fedorczac, F. Gensdarmes, C. Grisolia, B. Pégourié, E. Tsitrone, Micron-sized dust and nanoparticles produced in the WEST tokamak, Nuclear Materials and Energy 36 (2023) 101471. https://doi.org/10.1016/j.nme.2023.101471
21. M.K. Dosbolayev, A.B. Tazhen, A.N. Kholmirzayev, Y.A. Ussenov, T.S. Ramazanov: Studies of the formation and distribution of cracks and various defects on the heated tungsten plate surface during pulsed plasma flux impact, Nuclear Materials and Energy 37 (2023) 101540. https://doi.org/10.1016/j.nme.2023.101540

22. D. Papadakis, K. Mergia, E. Manios, V. Chatzikos, S. Dellis , D. Terentyev, G. Bonny, W. Van Renterghem, C.C. Chang, S.Messoloras, Defect evolution of neutron irradiated ITER grade tungsten after annealing, Fusion Engineering and Design 189 (2023) 113486. https://doi.org/10.1016/j.fusengdes.2023.113486
23. Chao Yin, Giovanni Bonny, Dmitry Terentyev, Anisotropy in the hardness of single crystal tungsten before and after neutron irradiation, Journal of Nuclear Materials 546 (2021) 152759. https://doi.org/10.1016/j.jnucmat.2020.152759
24. Michael Rieth, Russell Doerner, Akira Hasegawa, Yoshio Ueda, Marius Wirtz: Behavior of tungsten under irradiation and plasma interaction, Journal of Nuclear Materials 519 (2019) 334 – 368. https://doi.org/10.1016/j.jnucmat.2019.03.035
25. M. Shimada, R.A. Pitts, S. Ciattaglia, S. Carpentier, C.H. Choi, G. Dell Orco, T. Hirai, A. Kukushkin, S. Lisgo, J. Palmer, W. Shu, E. Veshchev, In-vessel dust and tritium control strategy in ITER, Journal of Nuclear Materials, 438 Supplement (2013) S996 – S1000. https://doi.org/10.1016/j.jnucmat.2013.01.217
26. G. Riva, P. Tolias, S. Ratynskaia, G. Daminelli, R. Donde, M. De Angeli, E. Vassallo, M. Pedroni, Adhesion measurements for tungsten dust deposited on tungsten surfaces, Nuclear Materials and Energy 12 (2017) 593 – 598. https://doi.org/10.1016/j.nme.2016.11.009
27. J.C. Flanagan, M. Sertoli, M. Bacharis, G. F. Matthews, P. C. de Vries, A. Widdowson, I. H. Coffey, G. Arnoux, B. Sieglin, S. Brezinsek, J. W. Coenen, S. Marsen, T. Craciunescu, A. Murari, D. Harting, A. Cackett, E. Hodille and JET-EFDA Contributors:, Characterising dust in JET with the new ITER-like wall, Plasma Physics and Controlled Fusion, 57, 1 (2015) 014037. https://iopscience.iop.org/article/10.1088/0741-3335/57/1/014037
28. D. Terentyev, M. Vilemova, C. Yin, J. Veverka, A. Dubinko, J. Matejicek: Assessment of mechanical properties of SPS-produced tungsten including effect of neutron irradiation, International Journal of Refractory Metals and Hard Materials 89 (2020) 105207. https://doi.org/10.1016/j.ijrmhm.2020.105207
29. J. Stoklasa, L. Karásková – Nenadálová, Possibility of processing waste tungsten dust from the nuclear fusion process by a combination of several technologies, Fusion Engineering and Design 191 (2023) 113505. https://doi.org/10.1016/j.fusengdes.2023.113505
30. K. Sihelská, D. Veselá, Tungsten particle analysis/measurement protocol, Verification of particle size distribution in Thermo 1μm sample, CVR (2023).
31. J. Lorinčík, et al., Identifikace a lokalizace dlouhodobých radionuklidů v environmentálních vzorcích pomocí SEM-EDX. SÚJB/OS/16315/ 2020, Certifikovaná metodika (2020). https://www.sujb.cz (accessed 12 March 2025)
32. I. Quintana, Z. Azpilgain, D. Pardo and I. Hurtado, Numerical Modeling of Cold Crucible Induction Melting, The Proceedings of the 2011 COMSOL Conference in Stuttgart (2011). https://www.comsol.com/paper/numerical-modeling-of-cold-crucible-induction-melting-11250
33. J. Stoklasa, J. Hrbek, L. Karásková Nenadálová, B. Mészáros, M. Paukov, Possibilities of Reprocessing Solid Waste with Tritium from Fusion Using High-Temperature Heating, Fusion Science and Technology 80, 3 – 4 (2024) 311. https://doi.org/10.1080/15361055.2023.2259227
34. A. Mühlbauer: Innovative Induction Melting Technologies, A Historical Revi, International Scientific Colloquium, Modelling for Material Processing June 8 – 9, Riga (2006).
35. M. Paukov, B. Mészáros, J. Hrbek, M. Kiselová, Investigation of Materials Interaction with Molten Corium - SI, Jaderná energie 1, 66 (2020) 66-68. https://jadernaenergie.online/wp-content/uploads/2020/09/CVR_casopis_jaderna_energie_S.pdf.
36. J. Hrbek, B. Mészáros, M. Paukov, M. Kudláč, Methodology for Measurement of Density of Liquid Oxides, ASME J of Nuclear Rad Sci. 7, 2 (2021). https://doi.org/10.1115/1.4048478
37. I. V. Andreyev, V. Petrovych, L. Georgyivna, Some Features of Sintering of Tungsten Powders, Science of Sintering 48, 2 (2016) 191. http://dx.doi.org/10.2298/SOS1602191A

Wolframový prach jako důležitý odpad z jaderného fúzního reaktoru

Jaroslav STOKLASA, Lucie KARÁSKOVÁ NENADÁLOVÁ

Centrum výzkumu Řež s.r.o. Hlavní 130, 250 68 Husinec-Řež

Souhrn

Jsou zkoumány zdroje wolframového prachu z procesu fúze a posuzuje se mechanismus jeho vzniku. V důsledku probíhajících procesů se v zařízeních souvisejících s jadernou fúzi uvolňují částice wolframu různých velikostí. Tento cenný odpadní materiál by měl být oddělen od radioaktivního tritia a recyklován. Ke koncentraci wolframu při současném odstranění tritia je možné použít buď technologii MSO (oxidace v roztavené soli), nebo alternativně indukční ohřev a tavení, případně jejich vhodnou kombinaci.

Klíčová slova: *wolfram; odpady, oxidace v roztavené soli (MSO), indukční ohřev (IH), velikost částic*